data statistics. In this window, statistical processing of experimental data are performed.

Developed system was tested on animals. As testing animals, the male Wistar rats aged 5 months were used. In these rats previously the conditioned food reflex was worked out. Studies of the dynamics of conditioned-reflex activity of rats in the experimental chamber were fulfilled using the developed Feeder system. The obtained numeric results are presented in Tab. 1. The designations of measured parameters correspond to those on Fig. 4. As can be seen from the Tab. 1 we measured parameters *RD*, *TRr*, *RN*, *RT* and *MI*. The data shows that rat took out the food in the average of two attempts (*RN*), the time of getting out of food was quite long and was about 1600 ms (*RD*). Also important to note the high activity of rat that tried to get the food at a time when the feeder was closed. The average number of such attempts was 14 (*MI*).

***Table* 1**

Numerical characteristics of the conditioned reflex of the rat

Parameter / attempt	RD, ms	TRr, ms	RN	RT, ms	MI
1	1750	0	1	1750	11
2	2016	0	1	2016	29
3	1969	251	5	2220	10
4	875	0	1	875	10
5	1489	327	2	1816	11
mean ± SE	1619 ± 208	116 ± 72	2 ± 1,7	1735 ± 230	14 ± 4

The data from the Tab. 1 were graphically presented in Fig. 5.

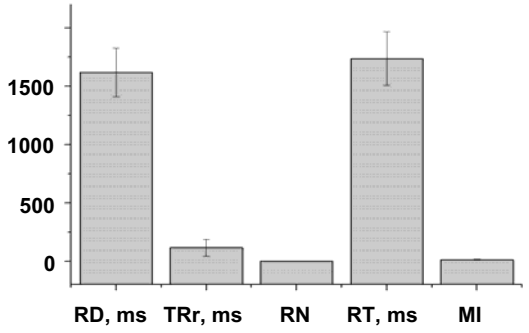

Fig. 5. Graphical representation of results

Conclusions. It was developed the automated registration system for registration of food behaviors of rats, analogues of which did not exist.

Testing of the system has shown its efficiency and effectiveness in the use of automated quantitative assessment of behavioral responses of rats.

The numerical parameters estimating the food conditioned reflex in rats were obtained with using the developed system.

REFERENCE:

1. *Bures J.* Techniques and basic experiments for the study of brain and behavior / *J. Bures, O. Bureshova, D. P. Houston* // Vysshaya Shkola, Moscow, 1991, – P. 216–220. (in Russian).

2. *Kostyk P.G.* Calcium ions in brain function – from physiology to pathology / *P. G. Kostyk, E. P. Kostyuk, E. A. Lukyanetz* // Kyiv: Naukova Dumka, 2005, – P. 99–152. (in Ukrainian).

Submitted on 09.10.14

Горбаченко В., студ., Череда І., студ.,
каф. медичної радіофізики, факультет радіофізики, електроніки та комп'ютерних систем,
Київський національний університет імені Тараса Шевченка
Врублевський С., пров. інж., Крученко Ж., канд. біол. наук, Лук'янець О., д-р біол. наук, проф.,
Інститут фізіології ім. О.О. Богомольця НАН України

РОЗРОБКА ТА ЕКСПЕРИМЕНТАЛЬНА АПРОБАЦІЯ СИСТЕМИ РЕЄСТРАЦІЇ ХАРЧОВОГО РЕФЛЕКСУ ЩУРІВ

Розроблено та створено автоматизовану систему для реєстрації поведінкової харчової реакції щурів. Система включає спеціалізоване обладнання та програмне забезпечення. Проведена апробація системи.

Ключові слова: *когнітивні здібності, харчовий рефлекс, щур, фотоелектрична реєстрація.*

Горбаченко В., студ., Череда И., студ., каф. медицинской радиофизики, факультет радиофизики, электроники и компьютерных систем,
Киевский национальный университет имени Тараса Шевченка
Врублевский С., вед. инж., Крученко Ж., канд. биол. наук, Лукьянец Е., д-р биол. наук, проф.,
Институт физиологии им. А. А. Богомольца НАН Украины

РАЗРАБОТКА И ЭКСПЕРИМЕНТАЛЬНАЯ АПРОБАЦИЯ СИСТЕМЫ РЕГИСТРАЦИИ ПИЩЕВОГО РЕФЛЕКСА КРЫС

Разработана и создана автоматизированная система для регистрации поведенческой пищевой реакции крыс. Система включает специализированное оборудование и программное обеспечение. Проведена апробация системы.

Ключевые слова: *крыса, когнитивные способности, пищевой рефлекс, фотоэлектрическая регистрация*

UDC 53; 547.136.13; 576.535; 577.037

A. Goriachko, Ph.D., P. Melnik, Ph.D., R. Sydorov, stud.,
O. Popova, stud., M. Nakhodkin, Dr.Sc., Acad. of NAS
Department Nanophysics and Nanoelectronics,
Faculty of Radiophysics, electronics and computer systems,
Taras Shevchenko National University of Kyiv

A NOVEL NANOPOSITIONING SYSTEM FOR SCANNING PROBE MICROSCOPY

We describe a new original design of the nano-positioning device to be used in scanning probe microscopy applications. It consists of four piezoelectric elements producing linear displacements, which are mechanically combined to obtain fully independent positioning capability along three orthogonal axes. The new device is ultra-compact, ultra-high vacuum compatible, and does not require any expensive parts to produce it. We report the results of preliminary testing of the scanning tunnelling microscope equipped with the novel nano-positioning system, which was used to obtain images of the graphite (0001) surface in ambient environment and the Ge(111) surface in ultra-high vacuum conditions.

Keywords: *scanning probe microscopy, piezoelectric effect, nano-positioning, ultra-high vacuum*

Introduction. Investigating matter at nano-scale is becoming ever more important in modern scientific endeavor. The nanostructures on solid surfaces can be researched in great detail by a group of techniques usually referred to as scanning probe microscopy (SPM). Among them are the scanning tunneling microscopy (STM) and the atomic force microscopy (AFM), which can routinely achieve atomic resolution on various solid surfaces.

All SPM techniques rely on the so-called "scanning" procedure, being essentially a controlled movement of a very sharp tip in a very close proximity to the surface of investigated sample. In order to obtain an image, one has to be able to move (scan) the tip independently in any orthogonal direction with a precision of ~0.01 nm. The easiest way to achieve this is to utilize an inverse piezoelectric effect, therefore, most SPMs are equipped with piezoelectric scanners. In Fig. 1, we summarize the previous known designs of piezoelectric scanners most often used in practical SPMs. They allow to move the probe tip relative to the investigated sample with the above mentioned precision, while a typical travel range is equal to several micrometers.

Historically, the first type of scanner was a tripod combination of three linear piezoelectric drives (Fig. 1a). These drives are attached to each other within the holder of the SPM probe tip, while their other sides are fixed to orthogonal reference planes. The simplest drive consists of a slab of some piezoelectric material with two of its opposing sides being covered by metal electrodes, to which a voltage can be applied. In this way, each individual drive can be independently elongated or contracted, thus moving the probe tip along the corresponding orthogonal axis. The linear drives are cheap and readily available, making the tripod scanner an easy option in SPM design. However, the tripod is problematic in terms of spatial limitations in ultra-high vacuum (UHV) microscopes, the latter being severely constrained by the inner diameter of the vacuum chamber flange.

The tube scanner (Fig. 1b) is by far the most often used type of scanner in modern SPMs. It consists of the piezoelectric material of the tubular shape, with inner and outer metallic electrodes, one end of the tube being fixed to the reference plane. The inner electrode is continuous, but there are four separate outer electrodes, each covering one fourth of the tube's outer perimeter. Normally, the inner electrode is grounded, so applying independent voltages to outer electrodes, one causes independent contraction or elongation of the tube's quarters. Inequivalent deformation of different quarters leads to bending of the entire tube. The direction of bending relative to the tube's axis is determined by voltage differences on the pairs of opposite outer electrodes. The magnitude of bending is negligible on the scale of tubes' dimensions, which is why such bending is equivalent to linear movement of the tube's free end in the plane perpendicular to the tube's axis.

This provides for the probe tip movement along two orthogonal axes (normally X, Y within the surface plane of the sample). Simultaneously, changing the average voltage on all four outer electrodes, leads to scanner's tube contraction or elongation as a whole, being equivalent to the movement of the tube's free end (where the probe tip is attached to) along the symmetry axis (normally Z axis perpendicular to the sample's surface).

Similar to the tube scanner in terms of the operation principle is the cross scanner (Fig. 1c). Instead of a tube, the piezoelectric material is shaped as a cross, which is extruded along the Z axis. One end of the scanner is firmly attached to the reference plane, while the other end (where the probe tip sits) is free to move according to actual deformations of the cross' four bars: X1, X2, Y1 and Y2. The latter can be addressed individually by applying voltages to their corresponding electrodes. Low magnitude bending of this scanner relative to its symmetry axis is equivalent to the movement of its free end within the plane, which is perpendicular to the axis (XY plane). Contraction or elongation of the scanner as a whole shifts its free end along the Z axis. In a nutshell, it is possible to set the XYZ coordinates of the scanner's free end in an arbitrary manner (within the maximum travel range) by setting the voltages on the X1, X2, Y1 and Y2 bars according to a specific algorithm.

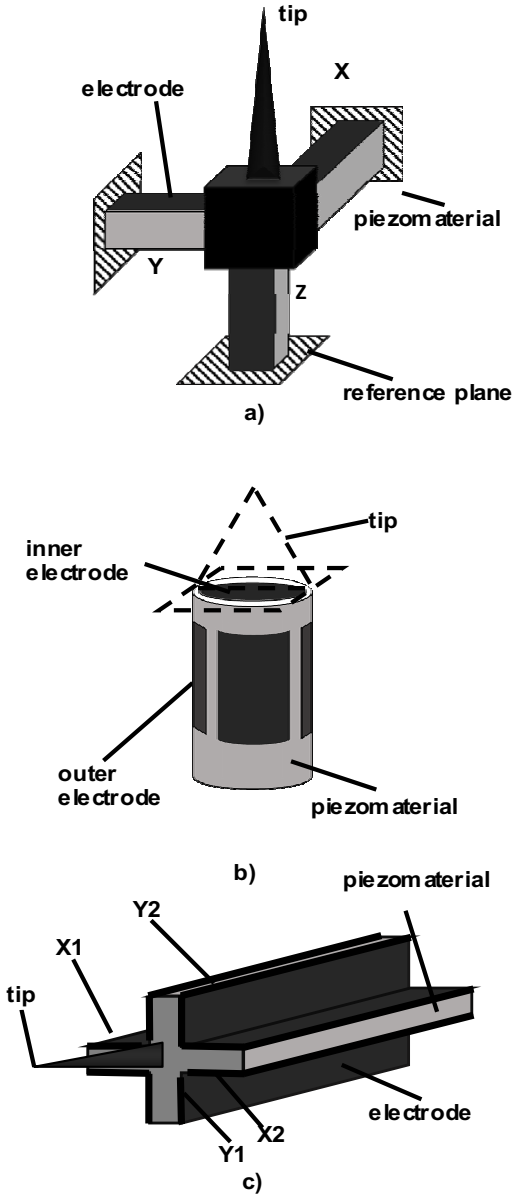

Fig. 1. Previously existing types of nano-positioning systems (scanners) for scanning probe microscopy:
a) tripod; b) tube ; c) cross

The tube and cross scanners are rather compact, thus being favorable for use in the UHV compatible SPMs. However, their production involves a sophisticated machining of the piezoelectric material, resulting in expensive devices. The major goal of the present work, was creation and testing of the new type of scanner, which would combine the compact shape of the cross scanner, but will be built as a combination of inexpensive linear piezoelectric drives.

Basic principles of the new nano-positioning system. The pivotal idea of the new nano-positioning device is to achieve a full three-dimensional positioning capability by combination of tilting with elongations or contractions. A proposed device (Fig. 2a) consists of the central cross-bar and the bridge (both made of stainless steel, aluminum, etc.) and four linear piezoelectric drives (similar to the ones used in the tripod scanner). A pair of two opposite drives has their lower ends glued to the reference plane, while their upper ends support the shoulders of the cross-bar. In its own turn, the lower part of the freely suspended cross-bar serves to support another orthogonal pair of linear drives. The latter are joined by the bridge above the cross-bar.

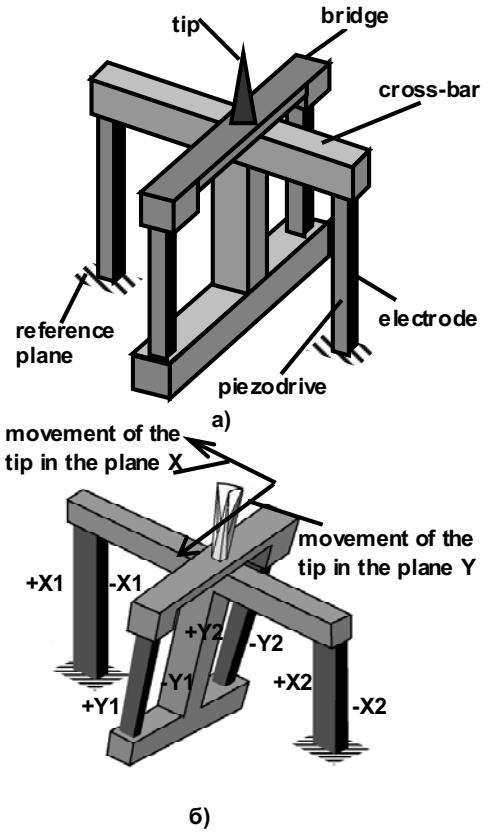

Fig. 2. The new proposed cross-bar type of scanner for nano-positioning in scanning probe microscopy:
a) general scheme of the scanner with the probe tip;
b) translation of tilting in different directions into linear movements of the tip within the XY plane of the sample's surface

The operation principle of the cross-bar scanner is depicted in Fig. 2b. If X drives are contracted/elongated to a different extent, the cross-bar becomes tilted together with another pair of drives and the bridge, which supports the SPM tip. As the magnitude of tilting is infinitesimal, it is equivalent to moving the tip along the X axis. If the Y drives are contracted/elongated to a different extent, only the bridge will be tilted, but in direction orthogonal to that described above. This is equivalent to the tip being moved along the Y axis. Finally, the tip's position along the Z axis is determined by the sum of average lengths of both pairs of piezoelectric drives.

In the following we describe the electrical addressing scheme of the piezodrives in the cross-bar scanner, which allows to set all three orthogonal coordinates of the tip independently (Fig. 3). The positive electrodes of all four piezodrives are connected together and biased by the UZ voltage source. The negative electrodes are biased separately by their respective voltage sources: UX1, UX2, UY1 and UY2. At any given value of UZ, the difference between UX1 and UX2 (or UY1 and UY2) will determine the X (or Y) coordinate of the tip. Also, changing the UZ at any given set of values UX1, UX2, UY1 and UY2 will change the Z coordinate of the probe tip.

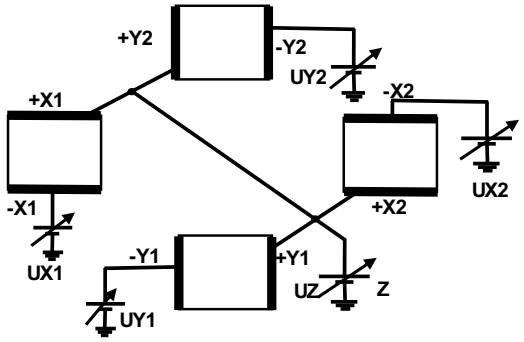

Fig. 3. Electrical addressing scheme of individual piezoelectric drives within the cross-bar scanner

The UX1 and UX2, or UY1 and UY2 are pairs of complementary voltages: if UX1 (UY1) is increased, then UX2 (UY2) is decreased correspondingly. This introduces unequal lengths within the X (Y) pair of piezoelectric drives and thus, tilting of the cross-bar and the bridge. In the limit of infinitesimal tilt, there is a linear dependence of X and Y coordinates on UX1, UX2, UY1 and UY2 voltages (Fig. 4). Due to the complementarity of the UX1 and UX2, or UY1 and UY2 voltages, their average remains constant. This leads to linear dependence of the tip's Z coordinate on the UZ voltage (Fig. 4). To avoid depolarization of the piezoelectric material, the minimum possible value of UZ must be higher than the maximum possible value of UX1, UX2, UY1 and UY2.

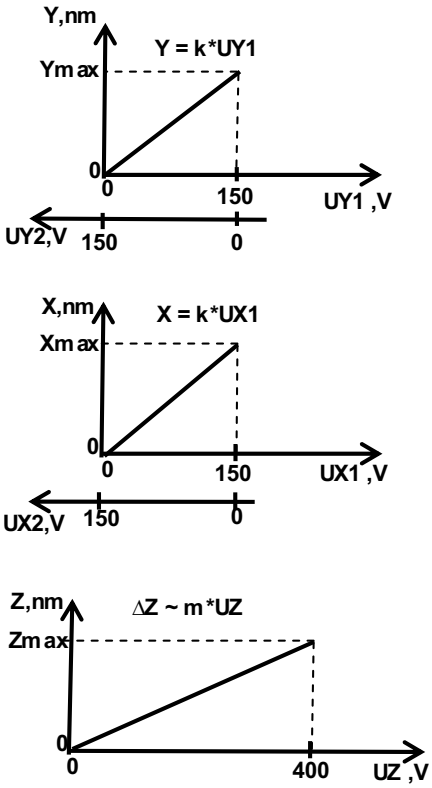

Fig. 4. Dependencies of X, Y and Z coordinates of the tip on the voltages supplied to the cross-bar scanner

Experimental. We have used simple home-made linear drives consisting of a PZT-type piezoelectric material (size: 14 mm x 1mm x 1mm) with two opposite sides covered by silver electrodes. They were glued to the cross-bar and the bridge by means of two-component UHV-compatible epoxy. This assembly was used as a scanner of a home-built STM mounted on the 6" conflate-type flange of the UHV chamber with the base pressure of $3x10^{-10}$ mbar. The UX1, UX2, UY1, UY2 and UZ voltages were supplied by the STM control unit, the maximum values of UX1, UX2, UY1 and UY2 being equal to 150 V, while the maximum value of UZ was equal to 400 V.

The scanner was tested for operation at 300 K in the ambient and UHV environments. The probe tip was hand-cut from the wire composed of 80% Pt and 20% Ir. Two samples were investigated: highly oriented pyro lithic graphite (HOPG) and p-type Ga-doped Ge(111). The fresh (0001) natural cleavage surface of HOPG was obtained by simple detachment procedure using the scotch tape. The Ge(111) wafer was cleaned in-situ by 500 eV Ar^+ ion bombardment and annealing at 900K.

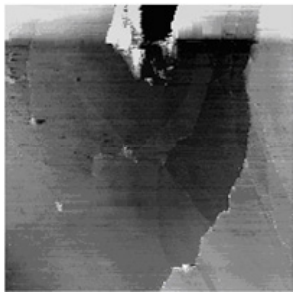

a)

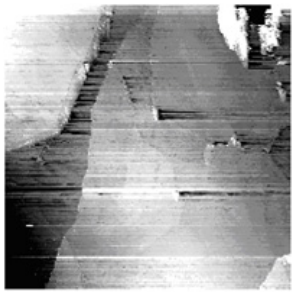

b)

c)

Fig. 5. a–c: Consecutive STM images of the HOPG(0001) surface.
The 1.5 μm x 1.5 μm imaged area is shifted from a) through c) due to thermal drift. Sample bias voltage U = 50 mV, tunneling current 5 nA.

The problem of rapid thermal drift is substantially reduced when the STM is operated in UHV, which improves the thermal isolation from the ambient environment. This is demonstrated by three consecutive images of the Ge(111) surface in Fig. 6a, 6b and 6c (image size 1.5 μm x 1.5 μm), with no substantial shifts of the imaged area. A smaller area (100 nm x 100 nm) on the same sample shows three atomically flat terraces separated by two single atomic steps (Fig. 7). Although atomic-size objects are plentiful on every terrace, no long range order is observed, indicating that the topmost layer of germanium sample is amorphous.

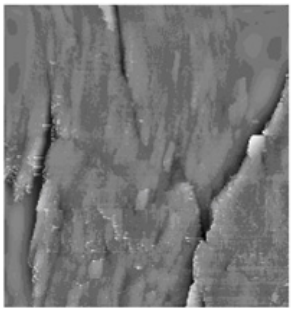

a)

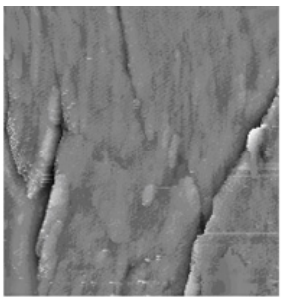

b)

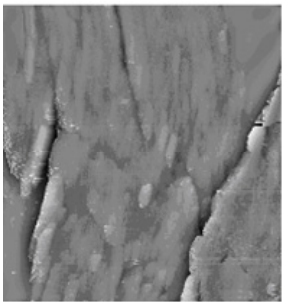

c)

Fig. 6. a-c: Consecutive STM images of the Ge(111) surface.
The image size is 1.5 μm x 1.5 μm, sample bias voltage U = 2.5 V, tunneling current I = 0.5 nA. No thermal drift is noticeable from a) through c).

Conclusions. In this work we have successfully designed and constructed a new type of the nano-positioning device (scanner) for applications in scanning probe microscopy. Its functioning was tested in the scanning tunneling microscope both in ambient and UHV environments. The obtained images of HOPG(0001) and Ge(111) show atomically flat terraces and single atomic steps.

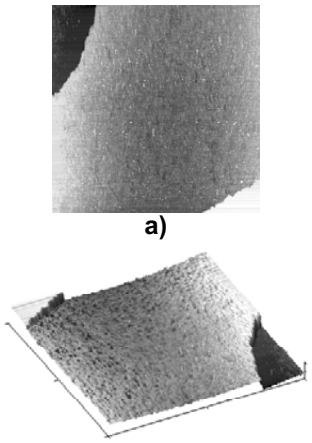

Fig. 7. STM images of the Ge(111) surface. The image size is 100 nm x 100 nm, sample bias voltage U = 2.5 V, tunnelling current I = 0.5 nA. a) grey-scale representation of the surface topography: brighter areas are closer to the viewer; b) 3D reconstruction of the surface topography.

REFERENCE:

1. *Elswijk H. B.* A model for Si molecular-beam epitaxy based on scanning tunneling microscopy observations and computer simulations. // H. B. Elswijk, A. J. Hoeven, E. J. van Loenen and D. Dijkkamp J. Vac. Sci. Technol. B, 1991. – Vol 9. – P. 451–455.

2. *Hambert P.K.* Scanning tunneling microscopy of surfaces and interfaces / P.K. Hambert // J. Micr. Electron., 1989. – V. 14. – P. 113–130.

3. A reliable compact ultra-high vacuum scanning tunneling microscope / *Lyubinetsky I.V.* et al. // Vacuum, 1995. – V. 46. – P. 219–222.

4. *Smith A. R.* A new high-resolution two-dimensional micropositioning device for scanning probe microscopy applications / *A. R. Smith, S. Gwo, and C. K. Shin* // Rev. Sci. Instrum., 1994. – V. 65. – P. 3216–3219.

5. *Wikramasinghe H. K.* Progress in scanning probe microscopy / H.K. Wikramasinghe // Acta material, 2000. – V.48. – P. 347–358

Submitted on 31.03.14

Горячко А., канд. фіз.-мат. наук, Мельник П., канд. фіз.-мат. наук,
Сидоров Р., студ., Попова О., студ., Находкін М., д-р фіз.-мат. наук, проф. акад. НАНУ
каф. нанофізики та наноелектроніки, факультет радіофізики. електроніки та комп'ютерних систем
Київський національний університет імені Тараса Шевченка

НОВІТНЯ СИСТЕМА НАНОПОЗИЦІОНУВАННЯ ДЛЯ СКАНУЮЧОЇ ЗОНДОВОЇ МІКРОСКОПІЇ

Описано новий оригінальний пристрій нанопозиціонування для застосування у скануючій зондовій мікроскопії. Пристрій складається з чотирьох п'єзо-електричних приводів лінійного переміщення, що механічно комбінуються в переміщення зонду скануючого мікроскопу уздовж трьох ортогональних осей у просторі. Така система є надкомпактною, сумісною із надвисоковакуумним обладнанням та не містить компонентів високої вартості. Попереднє тестування проводилося в скаунючому тунельному мікроскопі на поверхнях графіту (0001), у повітряному середовищі та германію (111), у надвисоковакуумному середовищі.

Ключові слова: *скануюча зондова мікроскопія, п'єзоелектричний ефект, нано-позиціонування, надвисокий вакуум.*

Горячко А., канд. физ.-мат. наук, Мельник П., канд. физ.-мат. наук,
Сидоров Р., студ., Попова О., студ., Находкин Н., д-р физ.-мат. наук, проф. акад.НАНУ
каф. нанофизики и наноэлектроники, факультет радиофизики, электроники и компьютерных систем
Киевский национальный университет имени Тараса Шевченко

НОВАЯ СИСТЕМА НАНОПОЗИЦИОНИРОВАНИЯ ДЛЯ СКАНИРУЮЩЕЙ ЗОНДОВОЙ МИКРОСКОПИИ

Описывается новое оригинальное устройство нанопозиционирования для применения в сканирующей зондовой микроскопии. Устройство состоит из четырех пьезоэлектрических приводов линейного перемещения, которые механически комбинируются в перемещения зонда сканирующего микроскопа вдоль трех ортогональных осей в пространстве. Такая система является сверхкомпактной, совместимой со сверхвысоковакуумным оборудованием и не содержит компонентов высокой стоимости. Предварительное тестирование проводилось в сканирующем туннельном микроскопе на поверхностях графита (0001), в воздушной среде и германия (111), в условиях сверхвысокого вакуума.

Ключевые слова: *сканирующая зондовая микроскопия, пьезоэлектрический эффект, нано-позиционирование, сверхвысокий вакуум.*

UDC 537.525:621.325

S. Denbnovetskiy, Dr. of Tech. Sc.,
I. Melnyk, Dr. of Tech. Sc., S. Tuhai, Ph.D.
Electronic Devices Department, Electronic Faculty,
National Technical University of Ukraine "KPI", Kyiv

ANALYTICAL RELATIONS FOR CALCULATION THE ENERGETIC EFFICIENCY OF TRIODE GLOW DISCHARGE ELECTRON GUNS

Dependences of energetic efficiency of triode high-voltage glow discharge electron guns from acceleration voltage, operation pressure and from voltage on additional electrode have been obtained and presented in the article. Obtained mathematical model is formed by analytical solving of algebraic equations, which is a result of consideration of equations of ions balance in anode plasma and equation of discharge self-consistency. Obtained simulation results are shown, that the energetic efficiency of triode glow discharge electron guns is lead in range 80–90%, therefore such type of electron guns can be successfully used in the modern electron-beam technologies.

Keywords: *electron guns, electron-beam technologies, high voltage glow discharge, anode plasma, triode electrode system*

Introduction. Glow discharge electron guns (GDEG) are widely used in industry for providing different technological operations, such as: effective, high-rate and high-quality welding in the soft vacuum; refusing of refractory materials; deposition of high-quality ceramics films and coatings in the soft vacuum; high-rate annealing of items in the soft vacuum [1, 2, 5, 6, 12–15]. Great interest to development and applying in industry of high voltage glow discharge (HVGD) electron guns is caused by many important advantages, which are difference such type of guns from the traditional